ResearchGate

See discussions, stats, and author profiles for this publication at: https://www.researchgate.net/publication/19076699

Thermodynamics and kinetics of phospholipid monomer-vesicle interaction

ARTICLE *in* BIOCHEMISTRY · DECEMBER 1985

Impact Factor: 3.02 · DOI: 10.1021/bi00344a011 · Source: PubMed

CITATIONS
84

READS
12

1 AUTHOR:

J. Wylie Nichols
Emory University
43 PUBLICATIONS **2,276** CITATIONS

SEE PROFILE

Available from: J. Wylie Nichols
Retrieved on: 25 January 2016

Thermodynamics and Kinetics of Phospholipid Monomer–Vesicle Interaction†

J. Wylie Nichols

Department of Physiology, Emory University School of Medicine, Atlanta, Georgia 30322

Received January 21, 1985

ABSTRACT: Resonance energy transfer between acyl chain labeled (7-nitro-2,1,3-benzoxadiazol-4-yl)-phosphatidylcholine (NBD-PC) and head group labeled (lissamine rhodamine B sulfonyl)phosphatidylethanolamine (*N*-Rh-PE) was used to monitor the rate of NBD-PC transfer between two populations of dioleoylphosphatidylcholine (DOPC) vesicles. Equilibration of NBD-PC between DOPC vesicles occurs by the diffusion of soluble monomers through the water phase, which is a first-order process. Conditions were used such that the apparent transfer rate constant is equal to the rate constant for monomer–vesicle dissociation into solution. The partition distribution of NBD-PC between DOPC vesicles and water was determined by measuring the loss of NBD-PC from vesicles into solution following the dilution of small amounts of vesicles in buffer. The acyl chain length and temperature dependence of both the rate and partition measurements were determined, and a free energy diagram for NBD-PC-soluble monomer–vesicle interactions was constructed. The conclusions of this analysis are the following: (1) NBD-PC dissociation from and association with the bilayer require passage through a high-energy transition state resulting predominantly from enthalpic energy. (2) The activation energy for NBD-PC–vesicle dissociation becomes more positive and the standard free energy of NBD-PC transfer from water to vesicles becomes more negative with increasing acyl chain length. (3) The standard free energy of transfer for NBD-PC from water to vesicles results predominantly from differences in enthalpy between the membrane and water phases. (4) The enthalpy of activation for association increases with acyl chain length and is larger than expected for an aqueous diffusion-limited process in bulk water.

Phospholipid molecules spontaneously transfer between different membranes and/or membranous particles with half-times ranging from 0.01 to 60 h depending on the phospholipid and membrane structure and temperature (Martin & McDonald, 1976; Papahadjopoulos et al., 1976; Duckwitz-Peterlein et al., 1977; Kremer et al., 1977a; Jonas & Maine, 1979; Roseman & Thompson, 1980; Nichols & Pagano, 1981, 1982; McLean & Phillips, 1981, 1984; Massey et al., 1982a,b; DeCuyper et al., 1983; Petrie & Jonas, 1984). In most of the systems studied, spontaneous transfer between membranes has been shown to occur through the aqueous phase via soluble monomer diffusion. In these cases, the monomer–membrane dissociation rate constant can be measured directly. However, a complete description of the transfer of monomers from membranes into solution requires measurement of either the monomer–membrane association rate constant or the equilibrium constant. Until now, a systematic study of this nature has not been made for long-chain phospholipids.

Equilibrium partitioning of acyl chain labeled (7-nitro-2,1,3-benzoxadiazol-4-yl)phosphatidylcholine molecules (NBD-PC)[1] between dioleoylphosphatidylcholine (DOPC) vesicles and water is measured by a new technique. Loss of NBD-PC from vesicles into solution (hence, the ratio of bound to free NBD-PC) is determined by resonance energy transfer between the NBD-PC molecule and a head group labeled *N*-(lissamine rhodamine B sulfonyl)phosphatidylethanolamine (*N*-Rh-PE) which is lost from the vesicles at a much slower rate. Kinetic measurements of the NBD-PC dissociation rate are made by a previously described technique (Nichols & Pagano, 1982) which also depends on resonance energy transfer between the two fluorescently labeled phospholipids. The combination of these two measurements with their respective dependence on temperature provides a complete thermodynamic and kinetic description of the transfer of a long-chain phospholipid (NBD-PC) from a phospholipid (DOPC) membrane into solution.

Experimental Procedures

Materials and Routine Procedures. DOPC, M-C_6-NBD-PC, P-C_6-NBD-PC, and S-C_6-NBD-PC (Figure 1) were purchased from Avanti Biochemical Corp., Birmingham, AL. *N*-Rh-PE was synthesized and purified as previously described (Struck et al., 1981). Lipids were stored at −20 °C, periodically monitored for purity by thin-layer chromatography, and repurified when necessary. Phospholipid concentrations were determined by a lipid phosphorus assay (Ames & Dubin, 1960).

Vesicle Preparation. Lipids were mixed in desired proportions and their storage solvents removed by evaporation under argon followed by a minimum of 4 h of vacuum desiccation. Vesicles were prepared by ethanol injection (Kremer et al., 1977b) as follows. The dried phospholipids were dissolved in ethanol (5 or 20 μmol/mL), injected into NaCl–HEPES at room temperature, and dialyzed against 4 L of

† This study was supported by U.S. Public Health Service Grant GM 32342 and an Emory University Research Grant.

[1] Abbreviations: NBD, 7-nitro-2,1,3-benzoxadiazol-4-yl; NBD-PC, 1-acyl-2-[6-[(7-nitro-2,1,3-benzoxadiazol-4-yl)amino]caproyl]phosphatidylcholine; M-C_6-NBD-PC, 1-myristoyl-2-[6-[(7-nitro-2,1,3-benzoxadiazol-4-yl)amino]caproyl]phosphatidylcholine; P-C_6-NBD-PC, 1-palmitoyl-2-[6-[(7-nitro-2,1,3-benzoxadiazol-4-yl)amino]caproyl]phosphatidylcholine; S-C_6-NBD-PC, 1-stearoyl-2-[6-[(7-nitro-2,1,3-benzoxadiazol-4-yl)amino]caproyl]phosphatidylcholine; *N*-Rh-PE, *N*-(lissamine rhodamine B sulfonyl)dioleoylphosphatidylethanolamine; *N*-NBD-PE, *N*-(7-nitro-2,1,3-benzoxadiazol-4-yl)dioleoylphosphatidylethanolamine; DOPC, dioleoylphosphatidylcholine; cmc, critical micelle concentration; NaCl–HEPES, 0.9% NaCl in 10 mM 4-(2-hydroxyethyl)-1-piperazineethanesulfonic acid, pH 7.4.

0006-2960/85/0424-6390$01.50/0 © 1985 American Chemical Society

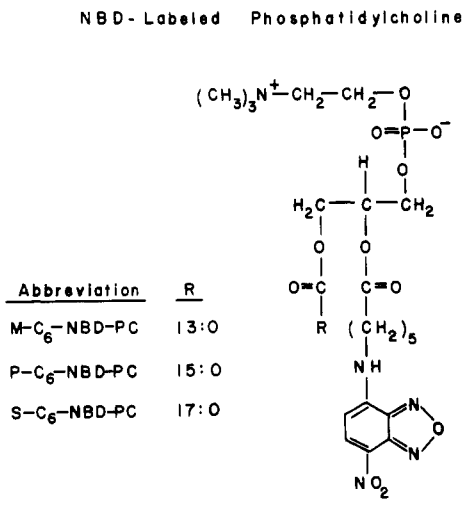

FIGURE 1: Structures of NBD-labeled phosphatidylcholines.

NaCl–HEPES overnight at 4 °C. The resulting vesicles (final concentration 250 or 1000 nmol/mL) were used on the day following injection.

Fluorescence Measurements. Fluorescence was measured with a Perkin-Elmer MPF-44E fluorescence spectrometer and was continuously recorded on a chart recorder. Peak absorbance of samples was kept to <0.1 to reduce inner filter effects. Solutions in the cuvette were stirred by a magnetic stirrer, and the temperature was controlled by a circulating water bath. Concentrations of NBD-labeled lipids and *N*-Rh-PE in vesicles were determined by disrupting the vesicles with Triton X-100 (1% final concentration) and measuring NBD and rhodamine fluorescence directly. Triton X-100 disruption eliminated energy transfer and allowed NBD-labeled lipid and *N*-Rh-PE concentrations to be determined by comparison to a standard curve made from stock solutions of fluorescent lipid.

Measurement of Dissociation Rate Constant from Vesicles. Resonance energy transfer between NBD-PC and *N*-Rh-PE was used to measure the rate of transfer of NBD-PC from donor to acceptor vesicles as described in detail previously (Nichols & Pagano, 1982). Briefly, the method is as follows. The fluorescence emission peak of NBD-PC overlaps the excitation peak of *N*-Rh-PE such that they are an efficient donor–acceptor pair for resonance energy transfer (Struck et al., 1981). Since the intervesicular transfer of *N*-Rh-PE is much slower than that of NBD-PC (Pagano et al., 1981; Struck et al., 1981), it can be used as a "nonexchangeable marker" to distinguish between donor and acceptor vesicles. When NBD-PC and *N*-Rh-PE are in the same vesicle, they are close enough so that when donor vesicle NBD-PC is excited, its emitted energy is transferred via resonance energy to *N*-Rh-PE and emitted at the rhodamine emission wavelength. Therefore, NBD-PC fluorescence is significantly quenched when the NBD-PC molecules remain in the *N*-Rh-PE-containing vesicles. The rate of NBD-PC transfer is measured by recording the rate of change of fluorescence following the addition of acceptor vesicles containing no fluorophore. The increase in fluorescence is directly proportional to the change in concentration of NBD-PC in the acceptor vesicles.

As previously described (Nichols & Pagano, 1982), the transfer of NBD-PC between phospholipid vesicles occurs via the diffusion of soluble monomers through the aqueous phase. The kinetics of intervesicular lipid transfer by this mechanism can be described by a model based on mass action kinetics (Nakagawa, 1974; Thilo, 1977; Nichols & Pagano, 1981, 1982). When both the donor and acceptor vesicles are composed of the same lipids (the assumption is made that the small percentage of fluorescent lipids in the vesicles does not significantly alter their bilayer properties), the model reduces to a simple first-order equation:

$$d[D]_I/dt = -k_{D-}[D]_I \quad (1)$$

where $[D]_I$ is the concentration of NBD-PC in the outer leaflet of the donor vesicles and k_{D-} is the off-rate constant from the vesicles. In other words, when these conditions are used, the off-rate constant can be obtained directly by measuring the rate of NBD-PC equilibration between vesicles. Selected experiments were plotted on a semilog plot in order to assure that the rate of equilibration was first order. Off-rate constants, however, were routinely calculated from measurements of the half-times for equilibration.

The off-rate constant for S-C_6-NBD-PC from homogeneous S-C_6-NBD-PC aggregates[2] was calculated from the initial rate of dequenching as these molecules moved from the highly self-quenched homogeneous aggregates to the nonquenching environment of DOPC vesicles (Nichols & Pagano, 1981).

Measurement of Vesicle–Water Equilibrium Partition. Measurements of the equilibrium partition of NBD-PC between the vesicle and water phases were made as follows. Small amounts of vesicles with the same phospholipid composition as the donor vesicles in the rate measurements (NBD-PC/*N*-Rh-PE/DOPC; mole ratio 4:1:95; 500 nmol/mL total phospholipid) were added to 2 mL of NaCl–HEPES buffer in a clean polystyrene cuvette, briefly stirred, and allowed to equilibrate. At relatively high concentrations of vesicle phospholipid (>5 nmol/mL for M-C_6-NBD-PC and >0.5 nmol/mL for P-C_6-NBD-PC) the amount of NBD-PC lost from the vesicle bilayer to solution is an insignificant fraction of the total. However, at very low concentrations of vesicle phospholipid (<0.5 nmol/mL for M-C_6-NBD-PC and <0.05 nmol/mL for P-C_6-NBD-PC), the amount of NBD-PC initially in the vesicles is small enough such that the amount lost to solution is a significant fraction of the total. The equilibrium partition is determined by measuring the distribution of NBD-PC between the vesicle and solution as described below.

At the concentrations of vesicles used in these experiments, insignificant amounts of *N*-Rh-PE are lost to solution (see control experiments described below). As a result, *N*-Rh-PE can be used to serve dual functions. First, the intensity of emitted light following the direct excitation of *N*-Rh-PE (excitation 580 nm; emission 610 nm) is linearly proportional to its concentration. It therefore provides a measure of the total vesicle phospholipid in the cuvette. Second, *N*-Rh-PE serves as an acceptor for resonance energy transferred from excited NBD-PC molecules. Since the NBD-PC and *N*-Rh-PE molecules must reside in the same vesicles for significant resonance energy transfer to occur, the intensity of light emitted by *N*-Rh-PE resulting from excitation of NBD-PC (excitation 475 nm; emission 610 nm) is linearly proportional to the concentration of NBD-PC residing in the vesicles. NBD-PC molecules in solution will not result in fluorescence emission at 610 nm. Thus, the emission of *N*-Rh-PE fluorescence at 610 nm excited at the *N*-Rh-PE excitation peak (580 nm) is proportional to the total phospholipid concentration and that excited at the NBD-PC excitation peak (475 nm) is proportional to the amount of NBD-PC residing in the vesicles. Since the concentrations of *N*-Rh-PE, NBD-PC, and

[2] Homogeneous aggregates of S-C_6-NBD-PC molecules are presumably in the form of bilayer vesicles although this structure has not been experimentally confirmed.

DOPC in the stock vesicles are known (see assay procedures above), the amount of NBD-PC initially in the vesicles can be calculated from the concentration of *N*-Rh-PE in the cuvette. The amount of NBD-PC in solution is equal to the amount added minus the amount residing in the vesicles after equilibration assuming that significant amounts of NBD-PC monomers do not adsorb to the cuvette walls or at the air–water interface.

The first possibility was tested by allowing the equilibrated vesicle solution to equilibrate a second time in a clean cuvette. If there was significant monomer sticking to the walls of the cuvette, additional NBD-PC would have been removed from the vesicles during a second equilibration and the ratio of NBD-PC to *N*-Rh-PE would further decrease. Monomer sticking was a significant problem when quartz cuvettes were used. The use of polystyrene cuvettes (Sarstedt) reduced the amount of monomer sticking to less than 10% of the amount in solution such that the amount of NBD-PC lost from the vesicles could be reasonably interpreted as that which is soluble in solution. The second possibility was tested by aspirating the surface of the equilibrated vesicle solution. No additional loss of NBD-PC from the vesicles occurred, indicating that the amount of NBD-PC monomer adsorption at the air–water interface was not a significant fraction of the amount in solution. Thus, the equilibrium distribution of the amounts of NBD-PC in vesicles and in solution at a given vesicle concentration can be determined by this method.

In order to demonstrate that *N*-Rh-PE is not lost from the vesicles at the vesicle concentrations used in these experiments, vesicle-containing head group labeled *N*-(7-nitro-2,1,3-benzoxadiazol-4-yl)phosphatidylethanolamine (*N*-NBD-PE) and head group labeled *N*-(lissamine rhodamine B sulfonyl)-phosphatidylethanolamine (*N*-Rh-PE) were prepared (*N*-NBD-PE/*N*-Rh-PE/DOPC; mole ratio 4:1:95; 500 nmol/mL total phospholipid), and the partition experiment described above was performed. Both of these probes have been shown to be stable in vesicles (Struck et al., 1981). With these vesicles the ratio of *N*-Rh-PE fluorescence excited by resonance energy transfer from *N*-NBD-PC and that excited directly remained constant with both peaks remaining directly proportional to vesicle concentration for vesicle concentrations as low as 2.5 pmol/mL total phospholipid (data not shown). Thus, an insignificant amount of *N*-Rh-PE is lost to solution in the vesicle concentration range used in these experiments. Therefore, *N*-Rh-PE can be used to quantify both the total amount of vesicle phospholipid and the amount of NBD-PC in the vesicles as described above.

Measurement of the Critical Micelle Concentration. Critical micelle concentrations were measured for M-C_6-NBD-PC, P-C_6-NBD-PC, and S-C_6-NBD-PC as previously described (Nichols & Pagano, 1981). Two hundred nanomoles of NBD-PC was dried under nitrogen and desiccated under vacuum. Two milliliters of NaCl–HEPES was added, and the solution was vigorously mixed. Serially smaller amounts of NBD-PC were added to a cuvette, and fluorescence was recorded (excitation 475 nm; emission 530 nm) and plotted. At low concentrations of NBD-PC the fluorescence increases as a linear function of concentration. As the concentration is increased, self-quenching aggregates begin to form and the fluorescence no longer increases linearly. The concentration at which self-aggregates begin to form is defined as the critical micelle concentration (cmc).

Measurement of Dissociation Rate Constant from Homogeneous Aggregates. The dissociation rate constant for homogeneous aggregates of S-C_6-NBD-PC was measured from initial rates of transfer as previously described (Nichols & Pagano, 1981). Initial rates of M-C_6-NBD-PC and P-C_6-NBD-PC were too rapid to be measured with the instrumentation available to the author. The initial rate of transfer was determined from the initial increase of fluorescence following the addition of excess acceptor DOPC vesicles to S-C_6-NBD-PC homogeneous aggregates. The initial transfer rate was quantified from a standard curve prepared for DOPC vesicles containing low concentrations of S-C_6-NBD-PC, and the dissociation rate constant was calculated from eq 1.

Calculation of the Equilibrium Constant. The equilibrium constant was determined by using the same model based on mass action kinetics derived to describe the diffusion of monomers between vesicles (Nichols & Pagano, 1981, 1982). Assuming the association rate is proportional to the product of the free monomer concentration and the surface area of the vesicles and the off-rate is proportional to its concentration on the surface, at equilibrium the association rate equals the dissociation rate and

$$k_{D-}[D]_I = k_{D+}[D]_m([A]_I s_A + [D]_I s_D)/1000 \quad (2)$$

where k_{D+} is the association rate constant for NBD-PC with units of cm s^{-1} and k_{D-} is the dissociation rate constant for NBD-PC with units of s^{-1}. $[D]_I$ is the concentration of NBD-PC in the outer leaflet of the vesicles (moles per liter of bulk solution). $[D]_m$ is the concentration of free monomers (M). $[A]_I$ is the concentration of DOPC in the outer leaflet of the vesicles (moles per liter of bulk solution). s_A and s_D are the surface area per mole of DOPC and NBD-PC, respectively (cm^2 mol^{-1}). Assuming s_A is equal to s_D, the equilibrium constant is defined as

$$K_{eq} = \frac{k_{D+}}{k_{D-}} \frac{s_A}{1000} \quad (3)$$

Then

$$K_{eq} = \frac{[D]_I}{[D]_m([A]_I + [D]_I)} \quad (4)$$

Previous experiments have shown that NBD-PC is distributed randomly between the inner and outer leaflets of the vesicle bilayer and that transverse bilayer movement (flip-flop) is slow (Nichols & Pagano, 1982). Thus, if a is defined as the fraction of total phospholipid that is in the outer leaflet, then

$$[A]_I = a[A]_T \quad (5)$$

and

$$[D]_m + [D]_I = a[D]_T \quad (6)$$

where $[A]_T$ is the concentration of total phospholipid in the vesicles per bulk solution (M) and $[D]_T$ is the total concentration of NBD-PC in bulk solution added to the cuvette. Substituting eq 5 and 6 into eq 4 and assuming $[D]_I \ll [A]_I$ give

$$K_{eq}[A]_T = \frac{[D]_T}{[D]_m} - \frac{1}{a} \quad (7)$$

Thus, if the ratio of $[D]_T$ to $[D]_m$ is determined for different concentrations of vesicle phospholipid, a plot of this ratio vs. total phospholipid is predicted to be linear with a slope equal to the equilibrium constant and a y intercept equal to the inverse of the fraction of total NBD-PC that is exposed to bulk solution.

Calculation of Standard Free Energy, Enthalpy, and Entropy for NBD-PC Transfer from Water to Vesicles. The standard free energy of transfer from water to vesicles

($\Delta G°_{w\to v}$) is defined as the difference in free energy for a solute residing in the vesicle phase and water, $\Delta G°_{w\to v} = \Delta G°_{v} - \Delta G°_{w}$. $\Delta G°_{v}$ and $\Delta G°_{w}$ are the differences in standard free energies of transfer for a solute between the gaseous and vesicle phases and the gaseous and water phases, respectively. The physical meaning of $\Delta G°_{w\to v}$ is the change in free energy on transferring 1 mol of solute from a hypothetical 1 molar aqueous solution to a hypothetical 1 molar lipid solution in which each solution has the physical properties of an infinitely dilute solution (Katz & Diamond, 1974a,b). The standard enthalpy of transfer, $\Delta H°_{w\to v}$, and the standard entropy of transfer, $\Delta S°_{w\to v}$, are defined analogously to $\Delta G°_{w\to v}$. The standard free energy of transfer is calculated from $\Delta G°_{w\to v} = -RT \ln K_{part}$. K_{part} is the molar partition coefficient and is obtained by dividing K_{eq} in eq 7 by the molar volume ($\bar{V}$) of DOPC molecules residing in a bilayer. $\bar{V}$ was estimated by using the molecular surface area of a monolayer of DOPC molecules at 12 dyn/cm presssure, 83 Å^2/molecule (O'Brien, 1967), and a length of 20 Å to be approximately 1.0 M^{-1}. The standard enthalpy and entropy of transfer are obtained from a van't Hoff plot of ln K_{part} vs. $1/T$ where the slope equals $\Delta H°_{w\to v}/R$ and the y intercept equals $\Delta S°_{w\to v}/R$. The temperature dependence of NBD-PC partition between the bulk solution and vesicle was measured repeatedly for only one concentration of vesicles at each temperature.

The values of $\Delta G°_{w\to v}$ and $\Delta S°_{w\to v}$ depend on the choice of concentration units, whereas $\Delta H°_{w\to v}$ is independent of the choice of units. In this work the molarity partition coefficient is used as opposed to the more common mole fraction partition coefficient.[3] $\Delta G°_{w\to v}$ (molarity) and $\Delta G°_{w\to v}$ (mole fraction) are related to K_{eq} as follows:

$$\Delta G°_{w\to v}\ (\text{molarity}) = -RT \ln (K_{eq}/\bar{V})$$

$$\Delta G°_{w\to v}\ (\text{mole fraction}) = -RT \ln K_{eq}(C_w)$$

Thus

$$\Delta G°_{w\to v}\ (\text{molarity}) - \Delta G°_{w\to v}\ (\text{mole fraction}) = RT \ln (\bar{V}C_w)$$

C_w is the molar concentration of water, 55 M, and the estimated $\bar{V}$ is 1.0 M^{-1}. Therefore, at 25 °C, $\Delta G_{w\to v}$ (molarity) = $\Delta G°_{w\to v}$ (mole fraction) + 2.4 kcal/mol. Since $\Delta H°_{w\to v}$ is independent of the concentration units, $T\Delta S°_{w\to v}$ (molarity) = $T\Delta S°_{w\to v}$ (mole fraction) − 2.4 kcal/mol at 25 °C.

Calculation of Activation Energies. Activation energies for monomer–vesicle dissociation were calculated by using a theoretical description of amphiphile monomer–micelle dissociation developed by Aniansson et al. (1976) from Kramers' theory of reaction rates (Kramers, 1940).[4] According to this theoretical description, the off-rate constant is predicted by the following relationship:

$$k_- = \frac{D_m}{(l_b)^2} \exp[-\Delta G^{‡°}_d/(RT)] \qquad (8)$$

where D_m is the diffusion constant for the exiting monomer, $\Delta G^{‡°}_d$ is the maximum energy barrier to monomer dissociation, l_b is the width of the barrier that is RT energy units below its maximum, and R and T are the gas constant and absolute temperature, respectively. This expression can be understood intuitively since $(l_b)^2/D_m$ is the time for diffusional motion over the distance l_b and $\exp[-\Delta G^{‡°}_d/(RT)]$ is the relative probability that a monomer resides in the region of length l_b or within RT energy units of $\Delta G^{‡°}_d$. The value for l_b was obtained by assuming that the free energy for dissociation is a linear function of the length of the monomer exposed to the bulk solution such that the ratio of l_b to l, the total length of the monomer, is equal to the ratio $RT/\Delta G^{‡°}_d$. Since $\Delta G^{‡°}_d$ is assumed to vary linearly with l, l_b remains relatively constant at approximately 0.7 Å for all three probe molecules used in these studies. D_m is assumed to be close to the diffusion constant of the free monomer in solution, and a value of 5×10^{-6} cm^2 s^{-1} was chosen as a reasonable estimate for molecules of this size.

At constant pressure, $\Delta G^{‡°}_d = \Delta H^{‡°}_d - T\Delta S^{‡°}_d$. Substituting into eq 8

$$\ln k_- = \frac{-\Delta H^{‡°}_d}{RT} + \frac{\Delta S^{‡°}_d}{R} + \ln [D_m/(l_b)^2] \qquad (9)$$

Therefore, $\Delta H^{‡°}_d$ can be determined from the slope of an Arrhenius plot of ln k_- vs. $1/T$, and $\Delta S^{‡°}_d$ can be determined from the y intercept.

Table I: Equilibrium and Kinetic Constants for NBD-PC Self-Aggregation at 25 °C

constant	units	phospholipid: M-C_6-NBD-PC	P-C_6-NBD-PC	S-C_6-NBD-PC
cmc[a]	M × 10^9	370	32	5
K_{eq}[b]	$M^{-1} \times 10^{-6}$	2.7	31	200
K_{part}[c]	$M^{-1} \times 10^{-6}$	3.2	32	185
$\Delta G_{w\to agg}$[d]	kcal/mol	−8.9	−10.2	−11.3
k_-^{NBD-PC}[e]	s^{-1}			0.027
$k_+S_A/1000$[f]	$M^{-1}\ s^{-1} \times 10^{-6}$			5.4
$\Delta G^{‡°}_d$[g]	kcal/mol			17.1
$\Delta H^{‡°}_d$	kcal/mol			13.2
$T\Delta S^{‡°}_d$	kcal/mol			−3.9

[a] cmc values were obtained from Figure 2. [b] According to eq 4, when D is the sole lipid, $K_{eq} = 1/[D]_m = 1/\text{cmc}$. [c] K_{eq} is converted to K_{part} by dividing by the molecular volume of NBD-PC. The molecular volume was estimated by assuming a constant molecular surface area of 83 Å^2 (O'Brien, 1967) and a length of 1.2 Å per carbon in the acyl chain. Molecular volume estimates are 0.84, 0.96, and 1.08 M^{-1} for M-C_6-NBD-PC, P-C_6-NBD-PC, and S-C_6-NBD-PC, respectively. [d] $\Delta G_{w\to agg} = -RT \ln K_{part}$. [e] The dissociation rate constant from NBD-PC homogeneous aggregates was determined from initial rate measurements. See Experimental Procedures for details. [f] $k_+s_A/1000 = (K_{eq})(k_-^{NBD-PC})$. [g] Activation energies for the dissociation rate constant were calculated from the Arrhenius plot in Figure 6 as described under Experimental Procedures.

Results

Critical Micelle Concentration. The cmc's for M-C_6-NBD-PC, P-C_6-NBD-PC, and S-C_6-NBD-PC are 370, 32, and 5 nM, respectively (Table I). These cmc values are compared with the literature values of cmc's for diacylphosphatidylcholines in Figure 2. The logarithm of the cmc is plotted vs. the effective number of carbons in the phosphatidylcholine molecule calculated as suggested by Tanford (Tanford, 1980, p 113), whereby the second acyl chain exerts an effect equivalent to 60% of that expected per carbon length in the first chain. This plots indicates that the acyl chain dependence of the cmc is the same for the NBD-labeled phosphatidylcholines as for the unlabeled molecules (cmc decreases approximately 2.8-fold per effective carbon). However, the NBD

[3] Although the choice of concentration units for thermodynamic analysis is arbitrary, Ben-Naim (1978) argues from a statistical mechanical level that the molarity scale is preferred.

[4] The Aniansson et al. model was chosen for kinetic analysis in this paper as opposed to the more general Eyring activated complex theory because it is based on a theoretical model derived for monomer–micelle interactions. Calculations using the Aniansson et al. model result in a standard free energy of activation 2.5 kcal/mol less, a standard enthalpy of activation 0.6 kcal/mol greater, and a standard entropy of activation 10.3 eu greater than the Eyring activated complex theory.

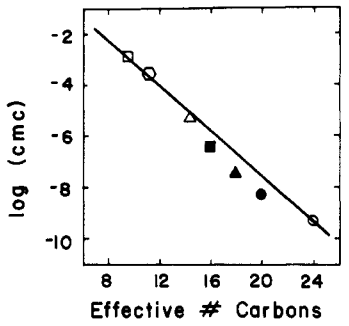

FIGURE 2: Comparison of critical micelle concentration at 25 °C of NBD-labeled phosphatidylcholine and diacylphosphatidylcholine. The solid symbols represent values for NBD-labeled phosphatidylcholines from Table I. (■) M-C_6-NBD-PC; (▲) P-C_6-NBD-PC; (●) S-C_6-NBD-PC. The open symbols represent literature values for diacylphosphatidylcholines: (□) diheptanoylphosphatidylcholine (Tausk et al., 1974); (○) dioctanoylphosphatidylcholine (Tausk et al., 1974); (△) didecanoylphosphatidylcholine (Reynolds et al., 1977); (○) dipalmitoylphosphatidylcholine (Smith & Tanford, 1972).

Table II: Kinetic and Thermodynamic Constants for NBD-PC Partitioning between DOPC Vesicles and Water at 25 °C

		phospholipid		
constant[a]	units	M-C_6-NBD-PC	P-C_6-NBD-PC	S-C_6-NBD-PC
K_{eq}	$M^{-1} \times 10^{-6}$	9.8 ± 2.1	94 ± 13	
k_{D-}	$s^{-1} \times 10^3$	349 ± 53	39.5 ± 1.1	3.86 ± 0.18
$k_{D+}s_A/1000$	$M^{-1}s^{-1} \times 10^{-6}$	3.4 ± 0.9	3.7 ± 0.5	
$\Delta G°_{w\to v}$[b]	kcal/mol	−9.6 ± 0.1	−10.9 ± 0.1	
$\Delta H°_{w\to v}$	kcal/mol	−7.1 ± 1.2	−8.2 ± 1.1	
$T\Delta S°_{w\to v}$	kcal/mol	+2.5 ± 1.1	+2.7 ± 1.0	
$\Delta G^{\ddagger}°_d$[c]	kcal/mol	+15.6 ± 0.0	+16.9 ± 0.0	+18.3 ± 0.0
$\Delta H^{\ddagger}°_d$	kcal/mol	+14.1 ± 0.6	+17.9 ± 0.8	+19.8 ± 0.3
$T\Delta S^{\ddagger}°_d$	kcal/mol	−1.5 ± 0.6	+1.0 ± 0.8	+1.5 ± 0.3
$\Delta G^{\ddagger}°_a$[d]	kcal/mol	+6.0 ± 0.1	+6.0 ± 0.1	
$\Delta H^{\ddagger}°_a$	kcal/mol	+7.0 ± 1.3	+9.7 ± 1.4	
$T\Delta S^{\ddagger}°_a$	kcal/mol	+1.0 ± 1.3	+3.7 ± 1.3	

[a] See Experimental Procedures for definition of constants. [b] Thermodynamic parameters derived from NBD-PC partitioning between DOPC vesicles and water at equilibrium. Average of four experiments. [c] Activation energies for NBD-PC dissociation from DOPC vesicles. Average of three experiments. [d] Activation energies for NBD-PC association with DOPC vesicles calculated by summing constants derived from both equilibrium and transfer rate measurements.

group shifts the line approximately 2.7 carbons to the left and therefore has the equivalent effect of increasing the length of the second acyl chain by approximately 4.5 carbons.

Monomer–Vesicle Dissociation Rate Constant Depends on Acyl Chain Length. The dissociation rate constant was measured for M-C_6-NBD-PC, P-C_6-NBD-PC, and S-C_6-NBD-PC, which differ only in the length of the acyl chain in the *sn*-1 position. Semilogarithmic plots of the amount of exchangeable probe remaining in the donor vesicles vs. time are linear and project through zero for all three phospholipids, indicating a single first-order transfer process (data not shown). The dissociation rate constant (k_{D-}) for each probe was calculated, and the results are presented in Table II. The magnitude of the dissociation rate constant decreases by a factor of approximately 3.2 per carbon increase in acyl chain length.

Vesicle–Water Equilibrium Distribution Is Dependent on Acyl Chain Length. The vesicle–water equilibrium constant was calculated from the slope of a plot of the ratio of total to free monomer NBD-PC concentration vs. DOPC concentration as described under Experimental Procedures (eq 7).

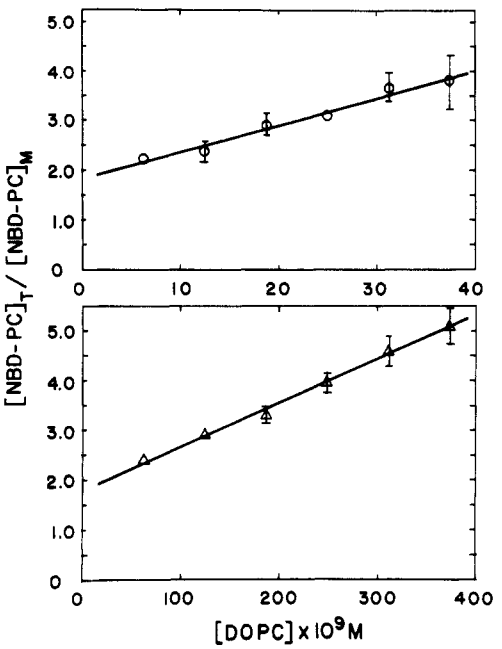

FIGURE 3: Ratio of total to water-soluble NBD-labeled phosphatidylcholine vs. concentration of DOPC vesicles. The circles (○) represent P-C_6-NBD-PC, and the triangles (△) represent M-C_6-NBD-PC. Note the different scales on the abscissa for each plot. See text for details.

The plots for M-C_6-NBD-PC and P-C_6-NBD-PC are shown in Figure 3 (the partition coefficient for S-C_6-NBD-PC is too large to be measured accurately by this technique). The plots for both probes are linear with similar *y* intercepts (approximately 1.8). Since the *y* intercept equals the inverse of the fraction of total NBD-PC exposed to the bulk solution, this indicates that 55% of the NBD-PC resides in the outer leaflet of the vesicles. The geometric constraints imposed upon the phospholipid molecules in small unilamellar vesicles result in a greater proportion of the total phospholipids residing in the outer leaflet of the vesicle bilayer (Johnson et al., 1975; Rothman & Dawidowicz, 1975; DiCorleto & Zilversmit, 1977; Nichols & Pagano, 1982). Therefore, these data are consistent with a random distribution of the probe molecules with DOPC molecules in which transbilayer movement (flip-flop) of the NBD-PC molecules is insignificant during the time of measurement. The linearity of these plots lends confidence that eq 7, which is based solely on soluble monomer–vesicle interactions, is the correct theoretical description for the equilibration of the NBD-PC molecules with phospholipid vesicles. If NBD-PC-soluble monomers were combining to form dimers or multimers, a curvilinear plot would be expected. The vesicle–water partition coefficients for M-C_6-NBD-PC and P-C_6-NBD-PC were calculated from the slopes of these plots. The magnitude of the partition coefficient increases with acyl chain length [K_{eq}(M-C_6-NBD-PC) = (9.8 ± 2.1) × 10^6 M^{-1} and K_{eq}(P-C_6-NBD-PC) = (9.4 ± 1.3) × 10^7 M^{-1}].

Calculation of the Association Rate Constant. The association rate constants for M-C_6-NBD-PC and P-C_6-NBD-PC were calculated by multiplying the measured dissociation rate constant by the respective equilibrium constant (eq 3) and are presented in Table II. The association rate constants are expressed in units of M^{-1} s^{-1} for ease of comparison with diffusion-limited transfer calculations to be discussed later. The association rate constant is independent of acyl chain length.

Dissociation Rate Constant Is Temperature Dependent. An Arrhenius plot of the temperature dependence of the disso-

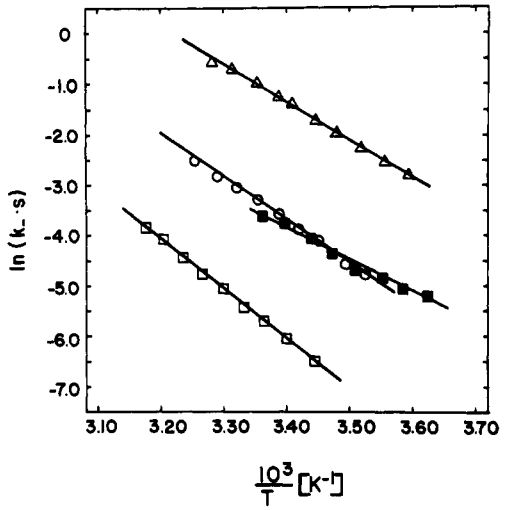

FIGURE 4: Representative Arrhenius plots of the dissociation rate constants for NBD-labeled phosphatidylcholines. The open symbols represent dissociation rate constants from DOPC vesicles and were calculated from the half-times of equilibration: (△) M-C_6-NBD-PC; (○) P-C_6-NBD-PC; (□) S-C_6-NBD-PC. The closed boxes (■) represent the dissociation rate constants from homogeneous aggregates of S-C_6-NBD-PC measured from initial rates of transfer. See text for experimental details.

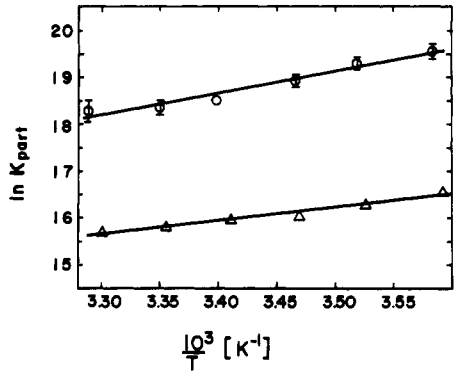

FIGURE 5: Representative van't Hoff plots of NBD-labeled phosphatidylcholine vesicle–water partition coefficient. The circles (○) represent P-C_6-NBD-PC and the triangles (△) represent M-C_6-NBD-PC. See text for experimental details.

ciation rate constant for M-C_6-NBD-PC, P-C_6-NBD-PC, and S-C_6-NBD-PC is presented in Figure 4. For each fluorescent phospholipid the semilog plot is linear, indicating that in the range of temperatures measured, the activation enthalpy is constant. These plots were used to calculate the enthalpy ($\Delta H^{\ddagger\circ}_d$), entropy ($\Delta S^{\ddagger\circ}_d$), and free energy ($\Delta G^{\ddagger\circ}_d$) of activation at 25 °C (Table II). The free energy of activation for dissociation increases between 0.65 to 0.7 kcal/mol per carbon added to the *sn*-1 acyl chain. For all three NBD-labeled phosphatidylcholine molecules, the magnitude of $\Delta G^{\ddagger\circ}_d$ is predominantly due to the enthalpy of activation, as the entropy of activation is relatively small.

Partition Coefficient Is Temperature Dependent. The temperature dependence of the vesicle–water partition coefficient for M-C_6-NBD-PC and P-C_6-NBD-PC was measured and is presented as a van't Hoff plot in Figure 5. According to the van't Hoff equation [$\ln K_{part} = -\Delta H^\circ_{w\to v}/(RT) + \Delta S^\circ_{w\to v}/R$], a plot of ln K_{part} vs. $1/T$ has a slope of $-\Delta H^\circ_{w\to v}/R$ and an intercept at $1/T = 0$ of $\Delta S^\circ_{w\to v}/R$. The values for $\Delta H^\circ_{w\to v}$ and $\Delta S^\circ_{w\to v}$ were calculated for M-C_6-NBD-PC and P-C_6-NBD-PC and are presented in Table II. The major component of the free energy difference for both molecules between the vesicle and water phases results from differences in enthalpy. The difference in entropy between the two states is small in both cases.

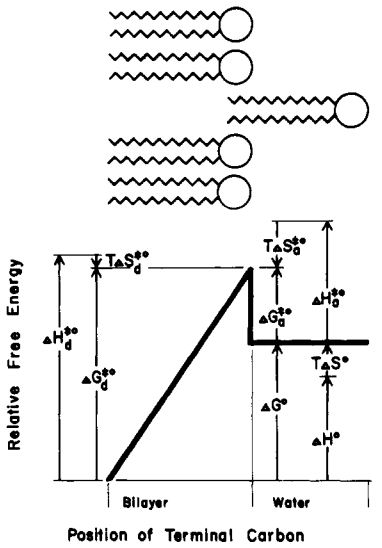

FIGURE 6: Free energy diagram of P-C_6-NBD-PC partitioning between DOPC vesicles and water. The upper schematic drawing represents a phospholipid molecule leaving a phospholipid bilayer. In the energy diagram below, the length and direction of the arrows represent the absolute magnitudes of the energy components.

Discussion

Kinetic and thermodynamic data for NBD-PC molecules interacting with DOPC vesicles are presented in this paper with the goal of gaining a better understanding of the forces that determine phospholipid vesicle stability. These fluorescent methods allow the measurement of both kinetic and equilibrium data for phospholipid molecules more hydrophobic (lower aqueous solubility) than have previously been measured, permitting a complete energetic description of phosphatidylcholine vesicle–water interaction. The NBD-PC molecules, although differing by the presence of the fluorophore from naturally occurring phosphatidylcholine molecules, self-aggregate to form micelles or bilayers with a dependence on acyl chain length similar to that measured for diacylphosphatidylcholines (Figure 2). This figure demonstrates that the polar and apolar regions of the NBD fluorophore combine to yield a net effect on the cmc equivalent to increasing the acyl chain length by 4.5 carbons. Thus, the net effect of the NBD group is to decrease the standard free energy of transfer from NBD-PC from water to homogeneous aggregates, $\Delta G^\circ_{w\to agg}$. The NBD group presumably has a similar effect on the free energy of transfer from water to vesicles, $\Delta G^\circ_{w\to v}$; however, it is not reasonable to assume that the relative contributions of enthalpy and entropy to the standard free energy of transfer upon addition of an NBD group will be equivalent to that expected by increasing the acyl chain length. By measurement of the acyl chain length dependence of each of the kinetic and thermodynamic parameters, the relative contribution of the acyl chain vs. the NBD fluorophore and choline head group can be determined. In this way, these fluorescent molecules can be used to predict the vesicle–water interactions of naturally occurring long-chain phospholipids. Data of this nature for unlabeled or radiolabeled long-chain phospholipids are technically difficult to obtain and are not available in the literature at this time.

A free energy diagram (Figure 6) was constructed from the data contained in Table II. The upper figure shows the schematic diagram of a single phospholipid molecule leaving a phospholipid monolayer. This diagram corresponds to the reaction coordinates used to develop the theoretical description

of this process (Aniansson et al., 1976). The molecule is considered to reside in the bilayer plane when its head group is in the same plane as its neighbors. The model assumes that the energy required to remove the phospholipid from the plane of the bilayer is a linear function of the fraction removed. The diagram is scaled to reflect the thermodynamic parameters for P-C_6-NBD-PC interaction with DOPC vesicles; however, the relative proportions of the diagram are similar for M-C_6-NBD-PC. The implications of this free energy diagram for phospholipid monomer–vesicle interactions are discussed below.

Standard Free Energy for NBD-PC Transfer from Water to Vesicles. The standard free energy of transfer from water to vesicles ($\Delta G°_{w\rightarrow v}$) becomes more favorable (negative) with increasing chain length. The difference in $\Delta G°_{w\rightarrow v}$ per added carbon for M-C_6-NBD-PC and P-C_6-NBD-PC, 0.65 kcal/mol, is consistent with that found for micellization of diacylphosphatidylcholine, 0.6 kcal/mol (see Figure 3 and Tables I and II). For both molecules, the dominant component of the free energy of transfer results from changes in enthalpy ($\Delta H°_{w\rightarrow v}$) and not entropy. This result is contradictory to the commonly held assumption that the partition of lipids from water into nonpolar solvents is driven by a positive entropy change (Tanford, 1980, p 77) and appears to be inconsistent with previous measurements of the relative contributions of enthalpy and entropy to the free energy of micellization of single-chain amphiphiles and short-chain diacyl lipids. For example, calorimetric measurements of micelle formation (Jones et al., 1971; Kresheck & Hargraves, 1974; Paredes et al., 1976; Johnson et al., 1981) and the temperature dependence of the cmc (Kresheck, 1975) give similar low values for the enthalpy of micellization (0 ± 2 kcal/mol). However, the enthalpy of transfer of hydrophobic molecules from water to an organic phase has been shown to decrease with increasing chain length [see Tanford (1980), p 24; Wishnia, 1963; Kresheck & Hargraves, 1974; Katz & Diamond, 1974a,b]. Katz & Diamond (1974a,b) measured a 0.72 kcal/mol decrease in the enthalpy of transfer of short-chain alcohols from water to dimyristoylphosphatidylcholine vesicles per added carbon. The decrease in $\Delta H°_{w\rightarrow v}$ of 0.55 kcal/mol per added carbon between M-C_6-NBD-PC and P-C_6-NBD-PC (Table II) is consistent. When the Katz and Diamond data are projected to longer chain alcohols, $\Delta H°_{w\rightarrow v}$ values for an effective acyl chain of 16 carbons (M-C_6-NBD-PC) and 18 carbons (P-C_6-NBD-PC) are −17.3 and −20.3 kcal/mol, respectively. Thus, a large favorable enthalpy of transfer from water to vesicles is not unexpected for the long-chain phospholipids used in this study. $\Delta H°_{w\rightarrow v}$ for M-C_6-NBD-PC and P-C_6-NBD-PC is more positive than that predicted from alcohols of equivalent chain length, due presumably to the more hydrophilic phosphorylcholine head groups.

The large favorable enthalpy of transfer from water to vesicles should not be assumed to reflect only a net attraction of the phospholipid molecules in the bilayer. A favorable enthalpy of transfer may also arise from changes in the enthalpy of the water phase. As defined above, the enthalpy of transfer for a solute from water to vesicles ($\Delta H°_{w\rightarrow v}$) is the difference between the enthalpy of transfer from the gaseous to vesicle phase ($\Delta H°_{v}$) and that from gaseous to water phase ($\Delta H°_{w}$). Various cavity models have been proposed to explain the partition of lipids between nonpolar and aqueous phases (Jenks, 1969; Pierotti, 1976) in which the energy required to create a suitably sized cavity is summed with the energy change resulting from the solution–solvent interaction. According to this model, the small enthalpy of transfer observed for small lipid molecules occurs because the unfavorable change in enthalpy required to move a cavity from the nonpolar phase to the water phase is offset by the favorable change in enthalpy resulting from the solute–solvent interaction in both phases. The large favorable enthalpy of association is observed for the longer chain phospholipids because the two sources of enthalpy change are no longer compensatory.

Although the degree to which the NBD fluorophore affects the enthalpy of transfer cannot be measured directly, the facts that (1) the enthalpy of transfer is dependent on the acyl chain length and (2) both the free energy and enthalpy of transfer are consistent with partition measurements of shorter chain amphiphiles argue strongly that the enthalpy of association is primarily due to interactions of the hydrophobic portion of these molecules with the water and vesicle phases and is not solely a consequence of the NBD group.

Activation Energy for NBD-PC Dissociation from Vesicles. The activation energy barrier to monomer–vesicle dissociation ($\Delta G^{\ddagger}°_{d}$) is much larger than the free energy difference between the two phases at equilibrium ($\Delta G°_{v\rightarrow w}$). This observation has been made previously for other amphiphiles (Doody et al., 1980; Pownall et al., 1983; McLean & Phillips, 1984) and is true regardless of whether the Aniansson et al. or the Eyring activated complex theory is used to calculate activation energies and regardless of whether the molarity or mole fraction partition coefficient is used to calculate the equilibrium free energy difference. The nature of the forces involved in forming the transition state are of particular interest since kinetic analysis of phospholipid transfer between membranes indicates that its rate of formation determines the rate of transfer (Roseman & Thompson, 1980; Massey et al., 1982a; Nichols & Pagano, 1981, 1982). McLean & Phillips (1984) proposed that the additional free energy, in excess of the free energy of transfer, required to form the transition state results from a decrease in entropy. By combining the temperature dependence data of both rate and equilibrium partition measurements, the relative contributions of enthalpy and entropy to the formation of the activated complex have been calculated (Table II and Figure 6). The data indicate that the entropy change upon formation of the activated complex is small or even positive. Thus, the activated complex results primarily from increases in enthalpy.

The schematic drawing in Figure 6 provides an illustration of how the cavity models of solvation can be used to provide a simplistic but useful interpretation of the nature of the activated complex in monomer–vesicle dissociation and association. The peak of the transition state is assumed to occur when the solute phospholipid has moved normal to the plane of the bilayer such that only the terminal carbon remains inserted. This is a high energy state because the remaining portion of the acyl chain does not allow collapse of the surrounding phospholipids to fill the cavity created by the exiting molecules. Thus, the transition state requires the creation of two cavities simultaneously, one in the bilayer and one in the water phase. Creation of a water-phase cavity presumably requires the energy to separate hydrogen-bonded water molecules whereas the energy opposing cavity creation in the bilayer arises from van der Waals interactions between the closely opposed phospholipid acyl chains and electrostatic interactions between the head groups. As the exiting molecule leaves the plane of the bilayer, the surrounding phospholipids collapse to fill the cavity resulting in a lower energy state.

According to this interpretation, the height of the activation barrier to dissociation and the magnitude of the dissociation rate constant is predicted to be dependent upon the combined

properties of the solute molecule, the membrane phase, and the water phase. This complex interdependence has been demonstrated for pyrene-labeled fatty acid movement between phospholipid vesicles (Doody et al., 1980), pyrene-labeled phospholipid movement between apolipoprotein recombinants (Massey et al., 1982a), and phosphatidylcholine movement between phospholipid vesicles (McLean & Phillips, 1984).

The free energy of activation for dissociation is dependent on the number and length of the solute acyl chains (Aniansson et al., 1976; Pownall et al., 1983) and the structure of the head group (Massey et al., 1982b; Nichols & Pagano, 1982; Pownall et al., 1983). The change in the free energy of activation for NBD-PC dissociation of 0.7 kcal/mol per added carbon (Table II) is consistent with these previous studies.

The free energy of activation for dissociation is dependent on the phase state of the bilayer (Doody et al., 1980; Massey et al., 1982a; McLean & Phillips, 1984). Dependence of the dissociation activation energy on the structure of the membrane phase is also illustrated by comparing the rate of dissociation of S-C_6-NBD-PC from DOPC vesicles (Table II) with that from homogeneous aggregates (Table I). The enthalpy of activation for the homogeneous aggregates is 6.5 kcal/mol less than for DOPC vesicles. However, this is compensated for by a decrease in entropy resulting in a decrease in the free energy of activation of only 1.2 kcal/mol giving a 7.2-fold increase in the dissociation rate constant. Furthermore, since the enthalpy and entropy for S-C_6-NBD-PC soluble monomers in solution ($\Delta H°_w$ and $\Delta S°_w$) are independent of the nonpolar phase, the enthalpy and entropy for S-C_6-NBD-PC in homogeneous S-C_6-NBD-PC aggregates ($\Delta H°_{agg}$ and $\Delta S°_{agg}$) must be less than that in DOPC vesicles ($\Delta H°_v$ and $\Delta S°_v$).

Rate of NBD-PC Association with Vesicles. The association rate constants for M-C_6-NBD-PC and P-C_6-NBD-PC are 3.4×10^6 and 3.7×10^6 M^{-1} s^{-1}, respectively. The molar units refer to the concentration of phospholipid residing in the outer leaflet of vesicles in bulk solution. When these units are converted to concentration of vesicles in solution by multiplying by a factor of 10^4 molecules/vesicle, obtained by assuming a vesicle diameter of 500 Å and a molecular surface area of DOPC of 83 $Å^2$, the association rate constants (3.4×10^{10} and 3.7×10^{10} M^{-1} s^{-1}, respectively) are of the magnitude expected for diffusion-limited rate processes in water (Gardner, 1969, pp 165–170). However, the enthalpy of activation for NBD-PC association with vesicles (7.0 and 9.7 kcal/mol for M-C_6-NBD-PC and P-C_6-NBD-PC, respectively) is significantly larger than that expected for a diffusion-limited process in bulk water at 25 °C (approximately 4.5 kcal/mol). This higher enthalpy of activation for association may result from diffusion through a structured layer of water at the vesicle interface or may arise from the energy required to break the electrostatic and van der Waals interactions that oppose cavity formation in the membrane.

The conclusions of this analysis are the following: (1) NBD-PC dissociation from and association with the bilayer requires passage through a high-energy transition state resulting predominantly from enthalpic energy. (2) The activation energy for NBD-PC–vesicle dissociation becomes more positive and the standard free energy of NBD-PC transfer from water to vesicles becomes more negative with increasing acyl chain length. (3) The standard free energy of transfer for NBD-PC from water to vesicles results predominantly from differences in enthalpy between the membrane and water phases. (4) The enthalpy of activation for association increases with acyl chain length and is larger than expected for an aqueous diffusion-limited process in bulk water.

ACKNOWLEDGMENTS

I thank Justyna Ozarowska for her technical assistance and Ron Abercrombie and Jim Bullock for critically reading the manuscript.

Registry No. M-C_6-NBD-PC, 98105-10-3; P-C_6-NBD-PC, 81005-34-7; S-C_6-NBD-PC, 98126-15-9; DOPC, 10015-85-7.

REFERENCES

Ames, B. N., & Dubin, D. T. (1960) *J. Biol. Chem. 235*, 769–775.

Aniansson, E. A. G., Wall, S. H., Almgren, M., Hoffman, H., Kielman, I., Ulbricht, W., Zana, R., Lang, J., & Tondre, C. (1976) *J. Phys. Chem. 80*, 905–922.

Ben-Naim, A. (1978) *J. Phys. Chem. 82*, 792–803.

DeCuyper, M., Joniau, M., & Dangreau, H. (1983) *Biochemistry 22*, 415–420.

DiCorleto, P. E., & Zilversmit, D. B. (1977) *Biochemistry 16*, 2145–2150.

Doody, M. C., Pownall, H. J., Kao, Y. J., & Smith, L. C. (1980) *Biochemistry 19*, 108–116.

Duckwitz-Peterlein, G., Eilenberger, G., & Overath, P. (1977) *Biochim. Biophys. Acta 469*, 311–325.

Gardner, W. C., Jr. (1969) *Rates and Mechanisms of Chemical Reactions*, W. A. Benjamin, Menlo Park.

Jencks, W. P. (1969) *Catalysis in Chemistry and Enzymology*, pp 393–436, McGraw-Hill, New York.

Johnson, L. W., Hughes, M. E., & Zilversmit, D. B. (1975) *Biochim. Biophys. Acta 375*, 176–185.

Johnson, R. E., Wells, M. A., & Rupley, J. A. (1981) *Biochemistry 20*, 4239–4242.

Jonas, A., & Maine, G. T. (1979) *Biochemistry 18*, 1722–1728.

Jones, M. N., Agg, G., & Pilcher, G. (1971) *J. Chem. Thermodyn. 3*, 801–809.

Katz, Y., & Diamond, J. M. (1974a) *J. Membr. Biol. 17*, 101–120.

Katz, Y., & Diamond, J. M. (1974b) *J. Membr. Biol. 17*, 121–154.

Kramers, H. A. (1940) *Physica (Amsterdam) 7*, 284.

Kremer, J. M. H., Kops-Werkhoven, M. M., Pathmamanoharan, C., Gijzeman, O. L. J., & Wiersema, P. H. (1977a) *Biochim. Biophys. Acta 471*, 177–178.

Kremer, J. M. H., v. d. Esker, M. W. J., Pathmamanoharan, C., & Wiersema, P. H. (1977b) *Biochemistry 16*, 3932–3935.

Kresheck, G. C. (1975) *Water: Compr. Treatise 4*, 95–167.

Kresheck, G. C., & Hargraves, W. A. (1974) *J. Colloid Interface Sci. 48*, 481–493.

Martin, F. J., & MacDonald, R. C. (1976) *Biochemistry 15*, 321–327.

Massey, J. B., Gotto, A. M., Jr., & Pownall, H. J. (1982a) *Biochemistry* 21, 3630–3636.

Massey, J. B., Gotto, A. M., Jr., & Pownall, H. J. (1982b) *J. Biol. Chem. 257*, 5444–5448.

McLean, L. R., & Phillips, M. C. (1981) *Biochemistry 20*, 2893–2900.

McLean, L. R., & Phillips, M. C. (1984) *Biochemistry 23*, 4624–4630.

Nakagawa, T. (1974) *Colloid Polym. Sci. 252*, 56–64.

Nichols, J. W., & Pagano, R. E. (1981) *Biochemistry 20*, 2783–2789.

Nichols, J. W., & Pagano, R. E. (1982) *Biochemistry 21*, 1720–1726.

O'Brien, J. S. (1967) *J. Theor. Biol. 15*, 307.

Pagano, R. E., Martin, O. C., Schroit, A. J., & Struck, D. K. (1981) *Biochemistry 20*, 4920–4927.

Papahadjopoulos, D., Hui, S., Vail, W. J., & Poste, G. (1976) *Biochim. Biophys. Acta 448*, 245-264.
Paredes, S., Tribout, M., Ferreira, J., & Leonis, J. (1976) *Colloid Polym. Sci. 254*, 637-642.
Petrie, G. E. & Jonas, A. (1984) *Biochemistry 23*, 720-725.
Pierroti, R. A. (1976) *Chem. Rev. 76*, 717.
Pownall, H. J., Hickson, D. L., & Smith, L. C. (1983) *J. Am. Chem. Soc. 105*, 2440-2445.
Reynolds, J. A. C., Tanford, C., & Stone, W. L. (1977) *Proc. Natl. Acad. Sci. U.S.A. 74*, 3796.
Roseman, M. A., & Thompson, T. E. (1980) *Biochemistry 19*, 439-444.
Rothman, J. E., & Dawidowicz, E. A. (1975) *Biochemistry 14*, 2809-2816.
Smith, R., & Tanford, C. (1972) *J. Mol. Biol. 67*, 75-83.
Struck, D. K., Hoekstra, D., & Pagano, R. E. (1981) *Biochemistry 20*, 4093-4099.
Tanford, C. (1980) *The Hydrophobic Effect: Formation of Micelles and Biological Membranes*, 2nd ed., Wiley-Interscience, New York.
Tausk, R. J. M., Karmiggelt, J., Oudshoorn, C., & Overbeek, J. Th. G. (1974) *Biophys. Chem. 1*, 175.
Thilo, L. (1977) *Biochim. Biophys. Acta 469*, 326-334.
Wishnia, A. (1963) *J. Phys. Chem. 67*, 2079.

Absorption Flattening in the Circular Dichroism Spectra of Small Membrane Fragments†

R. M. Glaeser* and B. K. Jap

Department of Biophysics and Medical Physics and Donner Laboratory, University of California, Berkeley, California 94720

Received March 25, 1985

ABSTRACT: The inhomogeneous distribution of chromophore occurring in a particulate suspension can result in a reduction in the apparent molar ellipticity recorded in circular dichroism (CD) spectra. The possibility of such a systematic error has often been a matter of concern when CD spectra of cell membrane proteins are recorded. The recent publication of CD spectra for bacteriorhodopsin in native and sonicated membranes, in detergent-solubilized form, and reconstituted into small unilamellar vesicles [Mao, D., & Wallace, B. A. (1984) *Biochemistry 23*, 2667-2673] gives a unique opportunity to apply the theoretical analysis of Gordon and Holzwarth [Gordon, D. J., & Holzwarth, G. (1971) *Arch. Biochem. Biophys. 142*, 481-488] so as to provide a definitive answer to the question of whether absorption flattening is significant for membrane particles. We show here that the data of Mao and Wallace can be combined with the theoretical analysis of Gordon and Holzwarth to rule out significant absorption flattening effects over the range 200-240 nm for submicrometer-sized membranes. In addition, the results show that absorption flattening can be disregarded even at 190 nm for membranous material in the size range below 100 nm. The demonstration that there are no major flattening effects in the CD spectra of bacteriorhodopsin, particularly in the region of 200-240 nm, means that the experimental spectra are incompatible with the proposal that this transmembrane protein contains seven transmembrane helices.

It has been proposed recently by Mao & Wallace (1984) that incorporation of membrane proteins into small unilamellar vesicles (SUVs) can provide a way to avoid certain errors in estimating secondary structure content from circular dichroism (CD) measurements. The number of protein molecules per vesicle can be made so small that the suspension must approach the homogeneous distribution of absorbers required in the derivation of Beer's law and the absorption flattening effect must theoretically vanish. The introduction of SUVs therefore represents a clever addition to the range of techniques that are available for spectroscopic studies of membrane proteins.

Mao and Wallace have also suggested that absorption flattening causes a significant distortion in the CD spectrum of both native and sonicated purple membrane and that the flattening effect causes a large error in estimating the α-helix content of the constituent protein, bacteriorhodopsin. We show here that this suggestion is actually inconsistent with the experimental data that the authors themselves present (Mao & Wallace, 1984). Furthermore, the suggestion that absorption flattening could cause significant distortions in the CD spectra of submicrometer-sized membrane sheets is inconsistent with both the theoretical analysis and the empirical estimation published by Gordon & Holzwarth (1971).

The accurate measurement of the molar amino acid concentration is essential in order to make an accurate comparison between the molar ellipticity of a specimen of unknown structure and that of the reference structures. Mao and Wallace introduced instead a procedure of spectral renormalization citing, as their justification, the difficulty of determining the concentration of membrane proteins. The renormalization procedure is not an adequate substitute for accurate biochemical determinations, however.

While absorption flattening effects can safely be dismissed when specimens are prepared as SUVs, the spectral curves obtained by Mao and Wallace show that more subtle shifts in spectroscopic wave form can still be produced in such

† This work was supported by the Director, Office of Energy Research, Office of Health and Environmental Research of the U.S. Department of Energy, under Contract DE-AC03-76SF00098 and by National Institutes of Health Research Grant GM22325.

* Address correspondence to this author at the Donner Laboratory, University of California, Berkeley.

0006-2960/85/0424-6398$01.50/0 © 1985 American Chemical Society